Oxygen diffusion, surface exchange and oxygen semi-permeation performances of Ln2NiO4+δ membranes (Ln = La, Pr and Nd)

Pierre-Marie Geffroy, Mickaël Reichmann, Thierry Chartier, Jean-Marc. Bassat, Jean-Claude Grenier

Oxygen diffusion, surface exchange and oxygen semi-permeation performances of $Ln_2NiO_{4+\delta}$ membranes (Ln = La, Pr and Nd)

P.-M. GEFFROY[1], M. REICHMANN[1,2], T. CHARTIER[1], J.-M. BASSAT[3] and J.-C. GRENIER[3]

[1] SPCTS, CNRS, ENSCI, Université de Limoges, CEC, 12 Rue Atlantis 87068 Limoges, France
[2] ADEME, 20 avenue du Grésillé, BP 90406, 49004 ANGERS Cedex 1, France
[3] CNRS, Université de Bordeaux, ICMCB, 87 Avenue du docteur Schweitzer, F-33608 Pessac, France

ABSTRACT

In order to clearly identify the rate determining step (rds) in oxygen semi-permeation of dense $Ln_2NiO_{4+\delta}$ membranes (with Ln = La, Pr and Nd), a specific setup has been designed, which allowed measuring the oxygen semi-permeation flux as well as the oxygen activity gradient at both membrane surfaces. From the results of the measurements, the coefficients of oxygen diffusion and surface exchange at both membrane surfaces have been determined. Their values have been compared with the values reported in the literature for similar membrane materials. The main conclusion is that the oxygen flux through these membranes is limited by the oxygen surface exchange at the oxygen-lean face, and not, as previously claimed, by oxygen volume diffusion.

Keywords: oxygen diffusion, oxygen surface exchange, oxygen semi-permeation, lanthanum nickelate.

Corresponding author:
Pierre-Marie GEFFROY
Affiliation : SPCTS, CNRS, ENSCI, Université de Limoges, CEC,
Adress: 12 Rue Atlantis 87068 Limoges, France,
phone: **05 87 50 23 53,**
Fax: **05 87 50 23 04,**
e-mail: pierre-marie.geffroy@unilim.fr

1. INTRODUCTION

The K_2NiF_4-type oxide materials are potential membrane materials for oxygen separation application, because of an excellent ionic conductivity and good kinetics of oxygen surface exchanges. This material series correspond to alkaline earth-free materials, of which lead to excellent chemical stability under CO_2 at high temperature, as confirmed in the recent works [1, 2]. The ionic transport in $Ln_2NiO_{4+\delta}$ based compounds, (Ln = La, Pr or Nd) occurs via an interstitial migration mechanism of oxygen anions [3-5]. These interstitial oxygen anions are incorporated in the structure into rock-salt LnO bilayers, and the electronic charge is compensated via the creation of holes located on Ni^{3+} cations in perovskite sheets formed by NiO_6 octahedra.

The partial substitution of Ln by Sr or Ca in the nickelate structure improves its chemical stability; nevertheless these substitutions lead to a decrease of oxygen semi-permeation or ionic conductivity [7, 8]. Hence, V.V. Vashhok *et al.* showed that among the $La_{2-x}Sr_xNiO_{4+\delta}$ compounds, $La_2NiO_{4+\delta}$ exhibits the highest oxygen semi-permeation [4]. However, the limiting step in oxygen transport through the $La_2NiO_{4+\delta}$ membranes has not been clearly identified. For instance, recent studies compared the coefficient of oxygen bulk diffusion obtained either by isotopic exchange method or by oxygen semi-permeation measurements [7-10]. The influence of the surface exchange kinetics in the oxygen flux through the membrane was often underestimated in these works. Consequently, the oxygen bulk diffusion is merely considered as the rate determining step in oxygen semi-permeation through the membranes.

For example, Mauvy *et al.* showed for $La_2Ni_{0.5}Cu_{0.5}O_{4+\delta}$ based membranes that the oxygen diffusion coefficients obtained from oxygen semi-permeation measurement are close to those obtained by isotopic exchange method [10]. However, these authors did not take into account the influence of the oxygen surface exchange on oxygen flux through the dense membrane. This assumes that the oxygen flux through $La_2Ni_{0.5}Cu_{0.5}O_{4+\delta}$ based membranes is governed by oxygen bulk diffusion, and not by oxygen surface exchange. Conversely, if the oxygen flux is governed by oxygen surface exchange, this approach leads to underestimate the oxygen diffusion coefficient values obtained by oxygen semi-permeation measurements.

Using oxygen permeation experiments, Kharton *et al.* recently showed that the oxygen flux is governed by the kinetics of oxygen exchange at the surface of $La_2NiO_{4+\delta}$ and $Pr_2NiO_{4+\delta}$ based membranes [9, 11]. The surface exchange involves a large gradient of the oxygen activity at the membrane surfaces (air and CH_4 atmospheres); however its slow kinetics prevents the decomposition of these materials under such conditions. To identify the rate determining step in the oxygen semi-permeation flux, the typical approach consists in evaluating the impact of the membrane thickness or additional porous layers on the oxygen flux through the membrane. In the same way, this work aims to identify the rate determining step in the oxygen flux through the $Ln_2NiO_{4+\delta}$ membranes (Ln = La, Pr and Nd). Such experiments require the use of a specific setup in which the oxygen activity (pO_2) gradient at both membrane surfaces is dissociated from the pO_2 gradient through the membrane thickness. Hence, the coefficients of oxygen bulk diffusion and of surface exchange on both membrane surfaces can be estimated and compared with the data obtained by isotopic exchange method [7-11].

2. EXPERIMENTAL PART

2.1 Preparation of membrane materials

The $Ln_2NiO_{4+\delta}$ membrane materials (Ln = La, Pr and Nd) were synthesized by nitrate-citrate route, as described in previous works [12-13]. The powders were finely attrition-milled using zirconia ball media in ethanol to obtain a monomodal grain size as small as 0.30-0.50 µm (Mastersizer 2000, Malvern Instruments). Then, they were qualitatively analysed using X-ray diffraction (D5000, Siemens).

The $Ln_2NiO_{4+\delta}$ membranes were shaped with the tape casting process, and more details about this shaping process have been reported in previous works [14, 15]. A 100 µm thick green tape was obtained after drying the casted tape. This green tape was cut into disk shape pieces that were stacked via a heat-lamination at

60 °C under 50 MPa. The green membranes had a relative density about 50% for $La_2NiO_{4+\delta}$ and 40% for $Pr_2NiO4_{+\delta}$ and $Nd_2NiO_{4+\delta}$. After debinding and a pre-sintering thermal treatment at 1150°C, the relative densities of $La_2NiO_{4+\delta}$, $Pr_2NiO_{4+\delta}$ and $Nd_2NiO_{4+\delta}$ membranes were 72, 83 and 53%, respectively. The stacks of green tapes were sintered to obtain dense membranes with 1 mm and 0.3 mm in thickness. The relative densities of sintered samples were measured by the Archimede method; the results are reported in Table 1. The sintering thermal treatment was optimized to obtain membranes with a maximal relative density of at least 95%. Microstructures of the nickelate membranes were observed by Scanning Electron Microscope (SEM S-2500, Hitachi), as shown in Figure 1.

As shown in Figure 1, the microstructures on cross sections of the $Ln_2NiO_{4+\delta}$ membranes evidence dense materials (≈ 95%) with a few residual porosity. The mean grain size in $La_2NiO_{4+\delta}$ and $Nd_2NiO_{4+\delta}$ membranes are very similar, close to 2-3 µm, while the microstructure of $Pr_2NiO_{4+\delta}$ membrane shows a smaller mean grain size, with 0.5-1 µm in diameter (Table 1). This is likely to result from the low sintering temperature (1250°C) of $Pr_2NiO_{4+\delta}$ membrane, which does not favour the granular growing. This small grain size may lead to a large impact on the oxygen flux through the membrane [16, 17], or on the oxygen surface exchange or oxygen diffusion coefficients. Unfortunately, no data has clearly been reported in the literature regarding the impact of the microstructure on the oxygen semi-permeation of nickelate membranes.
In addition, different $La_2NiO_{4+\delta}$ membrane designs were made thanks to a porous coating obtained by plating and drying a suspension on the membrane surface; this suspension consisted in a mixture of 40% vol. rice starch (Remy Industries NV, Belgium) and 60% vol. $La_2NiO_{4+\delta}$ powder in ethanol. The cohesive and porous coating was obtained after heat treatment at 1100°C under air for 1 hour (Fig. 2).

2.3. Measurements of the oxygen flux and of the oxygen activity at the membrane surfaces

The oxygen semi-permeation and the oxygen activities at the membrane surfaces were measured thanks to a specific setup presented in **Error! Reference source not found.**3 and described, with more details in a previous work [18]. A dense membrane of 1mm thick and 24 mm diameter was sealed between two alumina tubes using gold rings to obtain a tight system. Gas flow was imposed upon each opposite membrane faces (synthetic air to the bottom and argon to the upper surface), which causes an oxygen partial pressure gradient. In the temperature range from 600°C to 1000°C, with an interval of 25°C, the oxygen content in the argon sweep gas was monitored using an YSZ-oxygen sensor.

The oxygen flux through the membrane is evaluated from the following relationship, eq. 1.

$$J_{O_2} = \frac{f_{Ar}}{V_m}\frac{(P_{2out} - P_{2in})}{S} \qquad \text{eq. 1}$$

J_{O2} : the oxygen flux through the membrane in $mol.m^{-2}.s^{-1}$,
f_{Ar}: the argon flow in $l.s^{-1}$ (= $3.33\ 10^{-3}\ l.s^{-1}$),
V_m: the molar volume of argon in $l.mol^{-1}$ (= $24\ l.mol^{-1}$ at 20°C under 1 atm.),
S: the efficient membrane surface or membrane section (= $3.14\ 10^{-4}\ m^2$),
P_{2out}: the oxygen partial pressure in argon flux outlet,
P_{2in}: the oxygen partial pressure in argon flux inlet ($\approx 10^{-6}$).

The electromotive force, E_{sensor}, is given by YSZ-oxygen sensors used for the oxygen pressure measurement in argon flux outlet, P_{2out}, follows the Nernst law:

$$E_{sensor} = \frac{RT}{4F}\ln\frac{P_{2out}}{P_{O_2(air)}} \quad \text{or} \quad P_{2out} = P_{O_2(air)}\, e^{\frac{4F}{RT}E_{sensor}} \qquad \text{eq. 2}$$

with R, T and F the universal gas constant, temperature, and Faraday constant, respectively. $P_{O_2(air)}$ (with $P_{O_2(air)} = 0.21 \approx P_1 = P_{1out}$), and P_2 (with $P_2 = P_{2out}$), correspond, respectively, to the oxygen partial pressure in air, and the oxygen pressure in the flowing argon upstream or downstream the experimental setup.

In the investigated temperature range, the drop in di-oxygen activity between the membrane surface and the oxygen pressure in the gas can be measured thanks to the gold electrodes and the cone shaped microelectrodes made of 8 % yttria doped zirconia.

E_{s1} and E_{s2} correspond to electromotive forces due to the di-oxygen activity variation between the inlet gas and the oxygen-rich and oxygen-lean surfaces of the membrane, respectively. These two values are calculated from the Nernst law as follows:

$$E_{s1} = \frac{RT}{4F} \ln \frac{a_1}{a_1'} = \frac{\Delta\mu_{O2}^{surf(ox)}}{4F} \qquad \text{eq. 3}$$

$$E_{s2} = \frac{RT}{4F} \ln \frac{a_2'}{a_2} = \frac{\Delta\mu_{O2}^{surf(red)}}{4F} \qquad \text{eq. 4}$$

a_1 is the di-oxygen activity in air which is equal to the oxygen partial pressure P_1. Here, it has been checked that P_1, P_{1in} and P_{1out} are equal to 0.21.
a_1' is the di-oxygen activity on the oxygen-rich surface of the membrane.
a_2 is the di-oxygen activity in argon gas at the vicinity of the oxygen-lean surface, which is equal to the oxygen partial pressure noted P_{2out}. It is also assumed that the oxygen partial pressure of the gas outlet from argon chamber P_{2out} corresponds to one at the vicinity of the membrane surface.
a_2' is the di-oxygen activity on the oxygen-lean surface of the membrane.
$\Delta\mu_{O2}^{surf(ox)}$ and $\Delta\mu_{O2}^{surf(red)}$ are the gradients of the di-oxygen activity potential on the oxygen-rich and oxygen-lean surfaces of the membrane, respectively.

The electrochemical force through the membrane bulk, E_v, is calculated as a function E_{sensor}, E_{S1}, E_{S2}, and $\Delta\mu_{O2}^{bulk}$ as follows:

$$E_v = \frac{RT}{4F} \ln \frac{a_1'}{a_2'} = E_{sensor} - E_{s1} - E_{s2} = \frac{\Delta\mu_{O2}^{bulk}}{4F} \qquad \text{eq. 5}$$

$\Delta\mu_{O2}^{bulk}$ is the gradient of the di-oxygen chemical potential through the membrane volume region.

In previous works [18-20], the oxygen transport through oxide membranes has been decomposed into three main steps: 1) surface exchange on the oxygen-rich face, 2) oxygen diffusion through the membrane, and 3) surface exchange on the oxygen-lean face (Fig. 4).

The oxygen flux being governed by the slowest step (*i.e.* the rate determining step, r.d.s.), the knowledge of the oxygen chemical potential profile through the membrane allows directly identifying the r.d.s. of the oxygen flux through the membrane.

For instance, a large gradient of oxygen chemical potential through the membrane volume, $\Delta\mu_{O2}^{bulk}$, corresponds to oxygen flux governed by oxygen diffusion in the membrane. In this case, the thickness of the membrane governs directly the oxygen flux through the membrane. Conversely, a large gradient of oxygen chemical potential at the membrane surfaces corresponds to oxygen flux governed by oxygen surface exchanges.

3. Results

3.1. Rate determining step of the oxygen flux through the membrane

The Wagner's model being typically applied to describe the oxygen flux through a membrane bulk [18], hence, one can determine the oxygen diffusion coefficient using (eq. 6)

$$D_O = \frac{4RTL\,J_{O_2}}{C_O \Delta\mu_{O_2}^{bulk}} \qquad \text{eq. 6}$$

D_O is the self-diffusion coefficient of oxygen, L is the membrane thickness, C_O is the oxygen molar concentration in the membrane close to the membrane surfaces: it is evaluated from a previous work [6] (*cf.* annexe A).

$\Delta\mu_{O_2}^{bulk} = \mu_{O_2}^{surf(ox)} - \mu_{O_2}^{surf(red)}$ is the gradient of di-oxygen chemical potential in the membrane bulk region.

The relationship [eq. 6] is true only if the material is predominantly electronic conductor. This is the case for these materials which are characterized by a small ionic transport number (t_i), as reported in Tables 3 and 4.

However, the complete description of the oxygen transport through the membrane should take into account the oxygen exchange kinetics on both membrane surfaces. Kim *et al.* established the intrinsic material parameters, such as oxygen surface exchange coefficient using the well known Butler-Volmer formalism, as follows [21].

$$k_{ex}^{red} = 2J_{O_2} \Big/ C_O\left(\exp\left(\frac{n\mu_{O_2}^{surf(red)}}{RT}\right) - \exp\left(\frac{n\mu_{O_2}^{gas(red)}}{RT}\right)\right) \qquad \text{eq. 7}$$

$$k_{ex}^{ox} = 2J_{O_2} \Big/ C_O\left(\exp\left(\frac{n\mu_{O_2}^{gas(ox)}}{RT}\right) - \exp\left(\frac{n\mu_{O_2}^{surf(ox)}}{RT}\right)\right) \text{ if } \quad P_{O_2(g)} \approx P_{O_2(air)} \qquad \text{eq. 8}$$

For most of the mixed ionic and electronic conductors (MIEC), n is usually closed to 0.5 [22-24].

$\mu_{O_2}^{gas\,(ox)}$, $\mu_{O_2}^{gas(red)}$ are the oxygen chemical potentials in oxygen rich and oxygen lean gases, respectively. Thus, $\mu_{O_2}^{gas\,(red)} = RT\ln(P_{2out}/pO_{2\text{-}(air)})$ and $\mu_{O_2}^{gas\,(ox)} = RT\ln(P_{1out}/pO_{2\text{-}(air)}) = 0$ as $P_{1out} = pO_{2\,(air)} = 0.21$, which is the reference pressure corresponding to the oxygen partial pressure under air atmosphere.

$\mu_{O_2}^{surf\,(ox)}$, $\mu_{O_2}^{surf\,(red)}$ are the oxygen chemical potentials in the membrane at the vicinity of the surface in contact with oxygen rich and oxygen lean atmospheres, respectively. Thus, $\mu_{O_2}^{surf\,(ox)} = RT\ln(a_1'/a_{ref})$ and $\mu_{O_2}^{surf\,(red)} = RT\ln(a_2'/a_{ref})$ with $a_{ref} = pO_{2\,(air)} = 0.21$, which is the reference of oxygen chemical activity corresponding to the oxygen partial pressure under air atmosphere.

As a consequence of previous relationships, the variation of the oxygen flux as a function of the oxygen chemical potential gradient through the membrane surfaces is clearly not linear. The criterion of characteristic thickness (L_c) suggested by Bouwmeester, assuming a linear relation between the oxygen flux and the oxygen chemical gradient [20], cannot be applied in our case. Hence, L_c will not be taken into account in this work and is replaced by a novel criterion, namely B_c as previously reported in reference [25]. In this work it was shown that this criterion B_c is more relevant than the usual criterion L_c and it can be used to easily identify the rate determining step of the oxygen flux through the membrane [26].

It is expressed as follows: $B_c = \dfrac{\Delta\mu_{O_2}^{surfa}}{\Delta\mu_{O_2}^{Bulk}}$ eq. 9

It involves the oxygen chemical potential profile through the membrane as well as the oxygen chemical potential gradient at the surface.
From eq. 9, three cases are considered in this work (Table 2). For the first one, when $B_c >> 1$, the oxygen flux is governed by oxygen surface exchanges, and the second one, when $B_c << 1$, the oxygen flux is governed by oxygen diffusion. The third one, when B_c is close to unity, corresponds to a mixed regime, the oxygen flux being governed by both the bulk diffusion and the surface exchange kinetics.

In our case as well as for gas separation application, a large oxygen chemical gradient through the membrane leads to a large variation of oxygen exchange kinetics between both membrane surfaces, as suggested in eq. 7 and 8. Hence, it is required to distinguish each membrane surface in contrast to the usual model in which the surface exchange kinetics are similar on both membrane surfaces. In this way, it should be defined two criteria, B_c^{ox} and B_c^{red} for both the oxygen-rich and oxygen-lean surfaces of the membrane, respectively, as reported in Tables 3 and 4. It can be noticed that B_c^{red} is always higher than B_c^{ox}, and the conclusion deduced from L_c values can be contradictory with that obtained from B_c values. For example, for $La_2NiO_{4+\delta}$ à 800°C (Table 4), L_c values are close to 1 mm, which suggests that the oxygen flux is governed by a balance of volume diffusion and oxygen surface exchange. Conversely, B_c values are larger than unity on the oxygen-lean surface, which implies that the oxygen flux is governed by surface exchanges on the oxygen lean surface, and not by oxygen bulk diffusion.

Figure 5 shows the profiles of the oxygen chemical potentials through the three nickelate membranes. It is clearly evidenced that the drops of oxygen chemical potential are the largest on the oxygen-lean surface. This also suggests that the oxygen surface exchanges on oxygen-lean surface correspond to the rate determining step in oxygen transport through $Ln_2NiO_{4+\delta}$ membranes (Ln = La, Pr or Nd). This trend is even more pronounced for $Nd_2NiO_{4+\delta}$ membrane where the gradient of oxygen chemical potential at the oxygen-lean surface is higher than the ones obtained for $La_2NiO_{4+\delta}$ and $Pr_2NiO_{4+\delta}$ membranes. This may result from the specific microstructure of these membranes (Table 1), where a large grain size could be favourable to decrease the kinetics of surface exchange [17]. This corresponds here to an increase of B_c^{red} values from 1.0 and 2.4, to 3-3.2 in Table 3, for $Pr_2NiO_{4+\delta}$, $La_2NiO_{4+\delta}$, and $Nd_2NiO4_{+\delta}$ membranes at 900°C, respectively.

The coefficients of oxygen surface exchange and of oxygen diffusion were evaluated from oxygen potential drop at the membrane surfaces and the relationships eq. 6, 7 and 8. However, the values of oxygen surface exchange coefficients usually show a large scattering as a result of differences in the sample surface state [26]. This scattering of k_{ex}^{ox} values is often larger than the one of k_{ex}^{red} values, because the gradient of oxygen chemical potential is significantly lower at the oxygen-rich surface than the one at the oxygen-lean surface.

The Tables 3 and 4 report the oxygen diffusion and surface exchange coefficients, denoted D_O and k_{ex}, respectively, calculated from the oxygen flux and oxygen activity measurements at membrane surfaces. It assumes here that D_O and D* can be compared as the Haven ratio is equal to 1 for nickelate structure [30]. The values of D_O are in good agreement with D^* estimated from data obtained by Boehm *et al.* on these materials [6, 27], except for $Pr_2NiO_{4+\delta}$ at 900°C. However, a large spreading of D_O values is observed with oxygen semi-permeation measurements, particularly, at the lowest temperatures (< 800°C).

The $Pr_2NiO_{4+\delta}$ membranes at 900°C have oxygen fluxes 2 and 3 times higher than the ones of $Nd_2NiO_{4+\delta}$ and $La_2NiO_{4+\delta}$ membranes. Previous results obtained with $Ln_2Ni_{0.8}Cu_{0.2}O_{4+\delta}$ membranes showed similar trend, the $Pr_2Ni_{0.8}Cu_{0.2}O_{4+\delta}$ and $Nd_2Ni_{0.8}Cu_{0.2}O_{4+\delta}$ membranes exhibiting higher oxygen fluxes than the one of $La_2Ni_{0.8}Cu_{0.2}O_{4+\delta}$ membranes [31].

Concerning the surface exchange coefficients k, the sample surface morphology can explain the differences in their values. Indeed, a large roughness of the membrane surface may result in an increase of the effective values of k_{ex}. As far as the isotopic exchange method is concerned, the samples have been polished with alumina suspension or paste (0.25 μm), whereas the membranes used for oxygen semi-permeation

measurements have not been polished and likely show a higher surface roughness [32]. Therefore, the k_{ex} coefficients determined in this work are larger than the k* determined by isotopic exchange method.

In Tables 3 and 4, the B_c values suggest that the oxygen flux through nickelate membranes are governed by oxygen surface exchanges on oxygen-lean surface (*i.e.* in contact with argon atmosphere), although the L_c values correspond to a mixed regime where the oxygen flux is governed by a balance of oxygen bulk diffusion and surface exchanges. Kharton *et al.* [9, 11] confirmed that the oxygen flux through the $La_2NiO_{4+\delta}$ membranes with thicknesses of 1 mm is governed by the surface exchanges: this points out that B_c values are likely more relevant parameters than L_c values to identify the limiting step of the oxygen flux through a membrane, at least in these experimental conditions.

3.2 Influence of $La_2NiO_{4+\delta}$ membrane designs on the oxygen flux.

3.2.1 Semi-permeation measurements

In order to identify the rate determining step in the oxygen transport through a membrane, two ways have been selected. The first one consisted in varying the membrane thickness: if the oxygen flux is governed by surface exchanges, then the oxygen flux should not depend on it. The second one was to change the membrane designs using the addition of porous coatings in order to investigate the impact on the oxygen flux by modifying the oxygen surface exchanges. This study was only carried out on $La_2NiO_{4+\delta}$ membranes and not extended to $Pr_2NiO_{4+\delta}$ and $Nd_2NiO_{4+\delta}$; it was assumed that similar results would have been obtained, work is in progress

For this purpose, four membrane designs were made up, each design being identified by the following notation (as reported in Figure 6):

- LNO 1 corresponds to the typical membrane design with 1 mm thickness.
- LNO 0.3 corresponds to the membrane design with 0.3 mm thickness.
- LNO p-ox corresponds to the membrane design with 0.3 mm thickness and with a porous coating on the oxygen-rich surface (in contact with air flow).
- LNO p-red corresponds to the membrane design with 0.3 mm thickness and with a porous coating on oxygen-lean surface (in contact with argon flow).

The influences of the membrane thickness and porous coatings on the oxygen flux through the $La_2NiO_{4+\delta}$ membranes are depicted in Fig. 7. It clearly appears that a decrease of the thickness from 1 down to 0.3 mm has not significant impact on the oxygen flux through the $La_2NiO_{4+\delta}$ membrane. In addition, it is interesting to notice that Kharton *et al.* reported a similar behaviour and that the oxygen flux values for LNO 1 and LNO 0.3 membranes are in good agreement with its results [9] (Table 5).

On the other hand, thanks to the porous coatings deposited one of the faces of the membrane, the influence of the surface exchange kinetics on the oxygen flux shows that there is no significant impact on the oxygen flux for the LNO p-ox membrane, while the oxygen flux increases with a porous coating on the oxygen-lean surface (LNO p-red membrane). This suggests that the oxygen surface exchange at oxygen-rich surface is not the rate determining step of the oxygen semi-permeation through $La_2NiO_{4+\delta}$ membranes and that the oxygen flux is indeed governed by oxygen surface exchanges at the oxygen-lean surface. Actually, the additional porous coating increases the surface exchange kinetics, which results from an increase of the surface exchange area between gas and the membrane.

The inset in Fig. 7 shows the activation energy (Ea) of the oxygen flux through the membranes for the four designs. The activation energies are calculated in the range 700-900°C from the semi-permeation data of Fig. 6. These Ea values are reported in Table 5.

The Ea values of the oxygen flux measured for LNO 0.3 and LNO p-ox membranes are very close, 187 and 190 $kJ.mol^{-1}$, respectively. The Ea value for LNO 1 membrane is slightly lower than the previous ones (157 $kJ.mol^{-1}$). However, the predominant rate determining step of the oxygen flux is likely to be the same mechanism for these three membranes, as evidenced in Fig. 7.

Kharton *et al.* [9] have obtained similar values of the activation energy for $La_2NiO_{4+\delta}$ dense membranes, *i.e.* 155±2 kJ.mol^{-1}. On the other hand, Kilner *et al.* [28] have measured activation energy of the oxygen flux of about 180 kJ.mol^{-1} for similar membrane materials, which is very close to the Ea value determined for LNO 0.3 membrane. Unfortunately, the thickness of this membrane was not clearly mentioned.

Conversely, the Ea value of the oxygen flux through the LNO p-red membrane is significantly smaller compared to other membrane designs (102 kJ.mol^{-1} or 1.06 eV with regards to ≈ 190 kJ.mol^{-}1). This value could result from a mechanism involving rather oxygen bulk diffusion than surface exchange reaction. J. Maier gave an interesting viewpoint regarding the potential and fundamental mechanism about the oxygen surface exchanges in oxides [33]. This assumes that the predominant determining step is different for the LNO p-red membrane design; the next study is concerned with the oxygen chemical potential profiles and aims to confirm this assumption.

Finally, it can be noted in Tables 3 and 4 that the B_c^{red} values increase significantly when the temperature decreases, from 1.2-3.2 at 900° to 4-7.5 at 800°C for these nickelate membranes. This points out that the surface exchange on the oxygen-lean membrane face of LNO 1 is the rate determining step of oxygen transport through the membrane in the low temperature range (likely < 900°C), corresponding to a transport mechanism with larger activation energy. At higher temperature (close to or above 1000°C) the oxygen flux is likely to be governed by a mixed regime, as shown in Figure 8.

3.2.2 Oxygen chemical potential profiles through the $La_2NiO_{4+\delta}$ membranes

Figure 9 shows the profiles of the oxygen chemical potential (μ_{O2}) through the four $La_2NiO_{4+\delta}$ membranes using data of measurements of the oxygen activity at both membrane surfaces, as described in the previous section. The B_c^{ox} and B_c^{red} values calculated from the gradients of oxygen chemical potential allow easily identifying the rate determining step of the oxygen transport through the membranes (Table 7).

For LNO 1 membrane, the B_c^{red} criterion clearly confirms that the oxygen semi-permeation is mainly governed by the surface exchanges, as previously suspected. Then, the gradient of μ_{O2} is clearly more important on oxygen lean face than the one obtained on the oxygen-rich surface or through the membrane thickness.

The profiles of μ_{O2} through LNO 1, LNO 0.3 and LNO p-ox membranes are almost similar, with total gradient of μ_{O2} equal to - 40, - 42 kJ.mol^{-1} and - 45 kJ.mol^{-1}, respectively. One should stress that, LNO p-ox membrane exhibits a very low μ_{O2} gradient at the oxygen-rich surface (close to zero); it results from the porous coating that significantly increases the surface exchange area between air and the membrane. It clearly appears that the rate determining step of oxygen transport for LNO 1, LNO 0.3 and LNO p-ox membranes is the surface exchange at the oxygen-lean surface. This is in good agreement with the previous results regarding the impact of membrane design on the oxygen flux performances.

Conversely, the μ_{O2} profile through the LNO p-red membrane is somewhat different from those obtained for LNO 1, LNO 0.3 and LNO p-ox membranes. The μ_{O2} gradient at the oxygen-lean surface decreases significantly from 19-30 kJ.mol^{-1} down to 9 kJ.mol^{-1}, due to the porous coating on this surface. Hence, one can note that the B_c^{red} value decreases from 1.3 (for LNO 0.3 membrane) down to 0.5 (Table 5), which supposes that the oxygen flux through LNO p-red membrane is predominantly governed by oxygen bulk diffusion with a low contribution of surface exchanges on both membrane surfaces; B_c^{ox} or $B_c^{red} = 0.5$ or close to mixed regime.

In conclusion, the measurement of oxygen activity on both membrane surfaces allows a direct identification of the rate determining step for the oxygen flux through the membranes. Then, the oxygen flux can be easily improved with an appropriate membrane design. Indeed, it is observed an important change in the

predominant rate determining step between LNO 1 and LNO p-red membranes, corresponding to oxygen flux governed predominantly by surface exchanges and by bulk diffusion, respectively.

4. CONCLUSIONS

Measurements of the oxygen activity on both membrane surfaces of $Ln_2NiO_{4+\delta}$ membranes (Ln= La, Pr, Nd) showed that the oxygen flux through these membranes is mainly governed by the surface exchange on the oxygen-lean surface. The decrease of the membrane thickness from 1 to 0.3 mm has no impact on the oxygen flux through the $La_2NiO_{4+\delta}$ membranes. Hence, the increase of surface exchanges using porous coatings of $La_2NiO_{4+\delta}$ on the oxygen-lean surface leads to a significant increase of oxygen flux. The predominant rate determining step in the oxygen flux changes with a porous coating on the oxygen-lean surface, *i.e.* from surface exchange to bulk diffusion. Finally, the measurement of the oxygen activity on both membrane surfaces allows easily the identification of the rate determining step in oxygen flux through the membrane in using B_c^{ox} and B_c^{red} values.

The coefficients of oxygen diffusion and surface exchange obtained by semi-permeation have the same order of magnitude than those obtained by isotopic exchange method. This suggests that the approach presented in this work could be relevant for measuring the coefficients of oxygen diffusion and surface exchange close to the operating conditions of these membranes.

ACKNOWLEDGMENTS

The authors wish to express their gratitude to the ADEME (French Environment and Energy Management Agency) for financial support in this work.

REFERENCES

[1] T. Klande, K. Efimov, S. Cusenza, K.-D. Becker, A. Feldhoff, Effect of doping, microstructure, and CO2 on $LaNiO_{4+\delta}$-based oxygen-transporting materials, *J. Solid State Chem.* 184 (2011) 3310.

[2] J. Tang, Y.Y. Wei, L.Y. Zhou, J. Xue, Z. Li, H.H. Wang, Oxygen separation through U-shaped hollow fiber membrane using pure CO_2 as sweep gas, *AIChE J.* 58 (2012) 2473.

[3] S.J. Shinner, J.A. Kilner, Oxygen diffusion and surface exchange in $La_{2-x}Sr_xNiO_{4+\delta}$, *Solid State Ionics*, 135 (2000) 709

[4] V.V. Vashook, I.I. Yushkevich, L.V. Kokhanovsky, L.V. Makhnach, S.P. Tolochko, I.F. Kononyuk, H. Ullmann, H. Altenburg, Composition and conductivity of some nickelates, *Solid State Ionics,* 119 (1999) 23.

[5] V.V. Vashook, S.P. Tolochko, I.I. Yushkevich, L.V. Makhnach, I.F. Kononyuk, H. Altenburg, J. Hauck, H. Ullmann, *Solid State Ionics,* 110 (1998) 23.

[6] E. Boehm, J.M. Bassat, P. Dordor, F. Mauvy, J.C. Grenier, Ph. Stevens, Oxygen diffusion and transport properties in non-stoichiometric $Ln_{2-x}NiO_{4+\delta}$ oxides, *Solid State Sciences,* 176 (2005) 2717-2725.

[7] Z. Li, R. Hausgrud, T. Norby, Oxygen bulk diffusion and surface exchange in Sr-substituted $La_2NiO_{4+\delta}$, *Solid State Ionics,* 184 (2011) 42-46.

[8] Z. Li, R. Hausgrud, J.B. Smith, T. Norby, Transport properties and defect analysis of $La_{1.9}Sr_{0.1}NiO_{4+\delta}$, *Solid State Ionics*, 180 (2009) 1433-1441.

[9] A.L. Shaula, E.N. Naumovich, A.P. Viskup, V.V. Pankov, A.V. Kovalvsky, V.V. Kharton, Oxygen transport in $La_2NiO_{4+\delta}$: Assessment of surface limitations and multilayer membrane architectures, *Solid State Ionics*, 180 (2009) 812-816.

[10] F. Mauvy, E. Boehm, J.M. Bassat, J.C. Grenier, J. Fouletier, Oxygen permeation fluxes through $La_2Cu_{0.5}Ni_{0.5}O_{4+\delta}$ dense ceramics: Comparison with oxygen diffusion coefficients, *Solid State Ionics*, 178 (2007) 1200–1204.

[11] AV. Kovalesky, V.V. Kharton, A.A. Yaremchenko, Y.V. Pivak, E.V. Tsipis, S.O. Yakovlev, A.A. Markov, E.N. Naumovich, J.R. Frade, Oxygen permeability, stability and electrochemical behavior of $Pr_2NiO_{4+\delta}$ based materials, *J. Electroceram*, 18 (2007) 205-218.

[12] F. Mauvy, J.M. Bassat, E. Boehm, P. Dordor, J.C. Grenier, J.P. Loup, Chemical oxygen diffusion coefficient measurement by conductivity relaxation-correlation between tracer diffusion coefficient and chemical diffusion coefficient, *J. Euro. Soc.,* 24 (2004) 1265-1269.

[13] E. Boehm, J.M. Bassat, M.C. Steil, P. Dordor, F. Mauvy, J.C. Grenier, Oxygen transport properties of $La_2Ni_{1-x}Cu_xO_{4+\delta}$ mixed conducting oxides, *Solid State Sciences*, 5 (2003) 973-981.

[14] E. Juste, A. Julian, G. Etchegoyen, P.M. Geffroy, T. Chartier, N. Richet, P. Del Gallo, Oxygen permeation, thermal and chemical expansion of $(La,Sr)(Fe,Ga)O_{3-\delta}$ perovskite membranes, *J. Membr. Sci.*, 319 (2008) 185-191

[15] A. Julian, E. Juste, P.M. Geffroy, V. Coudert, S. Degot, T. Chartier, N. Richet, P. Del Gallo, Elaboration of $La_{0.8}Sr_{0.2}Fe_{0.7}Ga_{0.3}O_{3-\delta}/La_{0.8}M_{0.2}FeO_{3-\delta}$ (M = Ca, Sr and Ba) asymmetric membranes by tape-casting and co-firing, *J. Membr. Sci.*, 333, (1-2) (2009) 132-140.

[16] J. Martynczuk, M. Arnold, A. Feldhoff, Influence of grain size on the oxygen permeation performance of perovskite-type $(Ba_{0.5}Sr_{0.5})(Fe_{0.8}Zn_{0.2})O_{3-\delta}$ membranes, J. Membr. Sci., 322 (2008) 375–382.

[17] G. Etchegoyen, T. Chartier, A. Julian, P. Del-Gallo, Microstructure and oxygen permeability of a $La_{0.6}Sr_{0.4}Fe_{0.9}Ga_{0.1}O_{3-\delta}$ membrane containing magnesia as dispersed second phase particles, J. Membr. Sci. 268 (2006) 86.

[18] P.M. Geffroy, A.Vivet, J. Fouletier, N. Richet, P. Del Gallo, T. Chartier, Influence of oxygen surface exchanges on oxygen semi-permeation through $La_{(1-x)}Sr_xFe_{(1-y)}Ga_yO_{3-\delta}$ dense membranes, *J. Electrochem. Soc.*, 158 (8) (2011) 1-9.

[19] M. Guillodo, J. Fouletier, L. Dessemond, P. Del Gallo, Oxygen permeation through dense $Bi_2V_{0.9}Cu_{0.1}O_{5.35}$ ceramic membranes, *J. Electrochem. Soc.*, 149 (12) (2002) 93-99.

[20] H.J.M Bouwmeester, Dense ceramic membranes for methane conversion, *Catal. Today*, 82 (2003) 141.

[21] S. Kim, Y.L. Yang, A.J. Jacobson, B. Abeles., Oxygen surface exchange in mixed ionic electronic conductors membrane, *Solid State Ionics*, 121 (1999) 31-36.

[22] R.A. De Souza, A universal empirical expression for isotope exchange coefficients (k*) of acceptor-doped perovskite and fluorite oxides, *Physical Chemistry Physics*, 8 (2006) 890-897.

[23] R.H.E. Van Doorn, I.C. Fullarton, R.A. De Souza, J. Kilner, H.J.M. Bouwmeester, A.J. Burggraaf, Surface oxygen exchange of $La_{0.3}Sr_{0.7}CoO_{3-\square}$, *Solid State Ionics*, 96 (1997) 1-7.

[24] S. Kim, A. J. Jacobson, B. Abeles, Oxygen transport kinetics in $La_{0.6}Sr_{0.4}Fe_{0.8}Co_{0.2}O_{3-\square}$ membranes under both small and large oxygen partial pressure gradients, *Mat. Res. Soc. Proc.* 548 (1999).
[25] O. Valentin, E. Blond, N. Richet, Thermo-chemo-mechanical modelling of mixed conductors in transient stage, *Advances in Science and technology*, 65, (2010) 232-237.
[26] P.M. Geffroy, A.Vivet, J. Fouletier, C. Steil, E. Blond, N. Richet, P. Del Gallo, T. Chartier, The impact of experimental factors on the oxygen semi-permeation measurements, *J. Electrochem. Soc.*, 160 (1) (2013) F1-F9.
[27] E. Boehm, Thesis, Les nickelates $A_2MO_{4+\delta}$, nouveaux matériaux de cathode pour les piles à combustible SOFC moyenne température, University of Bordeaux, (2002).
[28] J.A. Kilner, C.K.M. Shaw, Mass transport in $La_2Ni_{1-x}Co_xO_{4+\delta}$ oxides with the K_2NiF_4 structure, *Solid State Ionics*, 154-155 (2002) 523-527.
[29] R. Sayers, R.A. Souza, J.A. Kilner, S.J. Skinner, Low temperature diffusion and oxygen stoichiometry in lanthanum nickelate, *Solid State Ionics*, 181 (2010) 386-391.
[30] Atom movements, diffusion and mass transport in solids. J. Philibert, Ed. de Physique (1991).
[31] S. Ziesche, R. Jurk, N. Trofimenko, M. Kusnezoff, Permeation and oxygen exchange of $Ln_2Ni_{0.8}Cu_{0.2}O_{4+\delta}$ materials (Ln= La, Pr, Nd), *Solid State Ionics,* 179 (2008) 1351-1353.
[32] J.M. Bassat, M. Petitjean, J. Fouletier, C. Lalanne, G. Caboche, F. Mauvy, J.C. Grenier, Oxygen isotopic exchange: a useful tool for characterizing oxygen conducting oxides, *Applied Catalysis A: General* 289 (2005) 84-89.
[33] S. B. Adler, X. Y. Chen, J. R. Wilson, Mechanisms and rate laws for oxygen exchange on mixed-conducting oxide surfaces, *Journal of Catalysis*, 245 (2007) 91-109.

Annexe A

δ_{air} and δ_{Ar} are the oxygen overstoichiometry amounts in the nickelate compounds under air (pO_2 = 0.21 atm) and argon atmosphere ($pO_2 \approx 10^{-5}$ atm). These values have been measured by thermogravimetry method under air (pO_2 = 0.21 atm) and nitrogen ($pO_2 \approx 10^{-5}$ atm).

C_O is the oxygen molar concentration in the membrane adjacent to the membrane surface. It is calculated using the relation: $C_O = 4*(4+\delta)/Vm$, Vm being the molar volume estimated from crystal cell parameters obtained by high temperature X-ray diffraction (data collected by Boehm [23]).

At 900°C	Vm ($Å^3$)	δ_{air}	δ_{Ar}	C_O (mol.cm^{-3}) at pO_2= 0.21 atm	C_O (mol.cm^{-3}) at $pO_2 \approx 10^{-5}$ atm
$La_2NiO_{4+\delta}$	390	0.12	0.08	$7.02\ 10^{-2}$	$6.95\ 10^{-2}$
$Pr_2NiO_{4+\delta}$	379	0.1	0.06	$7.19\ 10^{-2}$	$7.12\ 10^{-2}$
$Nd_2NiO_{4+\delta}$	372	0.155	0.115	$7.41\ 10^{-2}$	$7.34\ 10^{-2}$

Table 8: C_O, δ_{air} and δ_{Ar} values for $Ln_2NiO_{4+\delta}$ membranes at 900°C

At 800°C	Vm ($Å^3$)	δ_{air}	δ_{Ar}	C_O (mol.cm^{-3}) at pO_2= 0.21 atm	C_O (mol.cm^{-3}) at $pO_2 \approx 10^{-5}$ atm
$La_2NiO_{4+\delta}$	388	0.125	0.085	$7.05\ 10^{-2}$	$6.98\ 10^{-2}$
$Pr_2NiO_{4+\delta}$	377	0.11	0.07	$7.24\ 10^{-2}$	$7.17\ 10^{-2}$
$Nd_2NiO_{4+\delta}$	371	0.165	0.125	$7.46\ 10^{-2}$	$7.39\ 10^{-2}$

Table 9: C_O, δ_{air} and δ_{Ar} values for $Ln_2NiO_{4+\delta}$ membranes at 800°C

.

Tables

Table 1: Sintering thermal treatments and relative densities of the $Ln_2NiO_{4+\delta}$ membranes.

Table 2: Identification of the rate determining step of the oxygen flux from B_c values.

Table 3: The D_o and k_{ex} values at 900°C have been calculated from the relationships eq. 5, 6 and 9. D* and k* have been estimated from data of Boehm *et al.* [6, 27].

Table 4: The D_O and k_{ex} values at 800°C have been calculated from the relationships eq. 5, 6, 9 and data from refs. [3, 6, 27, 28, 29].

Table 5: Comparative values of the oxygen flux obtained with LNO 1 and LNO 0.3 membranes [9].

Table 6: Activation energy (Ea) of the oxygen flux through the $La_2NiO_{4+\delta}$ designed membranes.

Table 7: B_c^{ox} and B_c^{red} values for $La_2NiO_{4+\delta}$ membranes at 900°C.

Table 8: $C_{O,}$ δ_{air} and δ_{Ar} values for $Ln_2NiO_{4+\delta}$ membranes at 900°C

Table 9: $C_{O,}$ δ_{air} and δ_{Ar} values for $Ln_2NiO_{4+\delta}$ membranes at 800°C

Figures

Figure 1: Microstructures on cross sections of the dense $Ln_2NiO_{4+\delta}$ membranes with a) Ln = La, b) Ln = Pr and c) Ln = Nd.

Figure 2: Microstructures on cross section of the dense $La_2NiO_{4+\delta}$ membranes with porous layer of 5 µm in thickness.

Figure 3**:** Schematic diagram of the setup for the oxygen semi-permeation flux measurement including the oxygen activity measurement at both membrane surfaces [18].

Figure 4: Schematic representation of the oxygen chemical potential gradient through the membrane showing the three main steps of oxygen transport.

Figure 5: Profiles of the oxygen chemical potentials through the nickelate membranes: a) $La_2NiO_{4+\delta}$, b) $Pr_2NiO_{4+\delta}$ and c) $Nd_2NiO_{4+\delta}$ at 900 °C.

Figure 6: Representation of the various $La_2NiO_{4+\delta}$ membrane designs.

Figure 7: Influence of the membrane thickness and of the porous coatings on the oxygen flux through the $La_2NiO_{4+\delta}$ membranes.

Figure 8: Rate determining step identification of the oxygen flux through $La_2NiO_{4+\delta}$ dense membrane (LNO 1) using the thermal variation of B_c^{ox} and B_c^{red} values.

Figure 9: Profiles of the oxygen chemical potentials through $La_2NiO_{4+\delta}$ membranes with various designs at 900 °C: a) LNO 1, b) LNO 0.3, c) LNO p-ox and d) LNO p-red.

Figure 1
Click here to download high resolution image

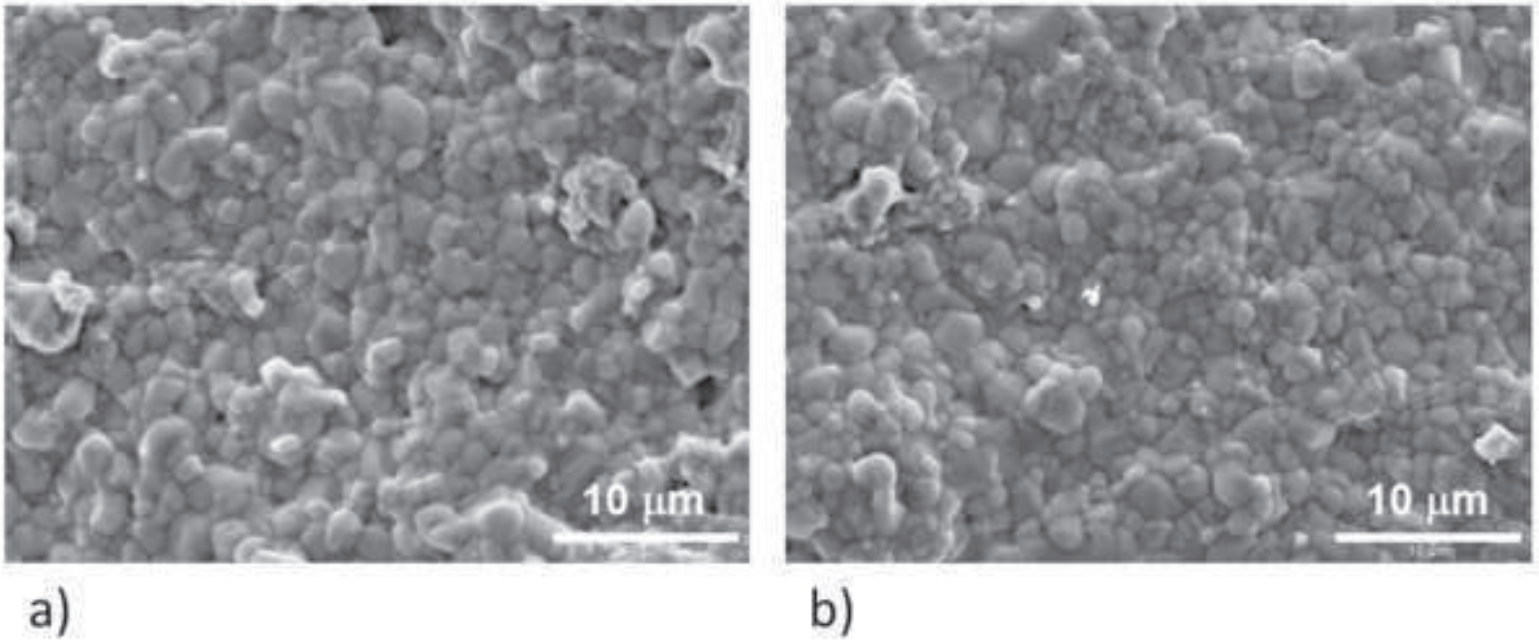

Figure 2

Click here to download high resolution image

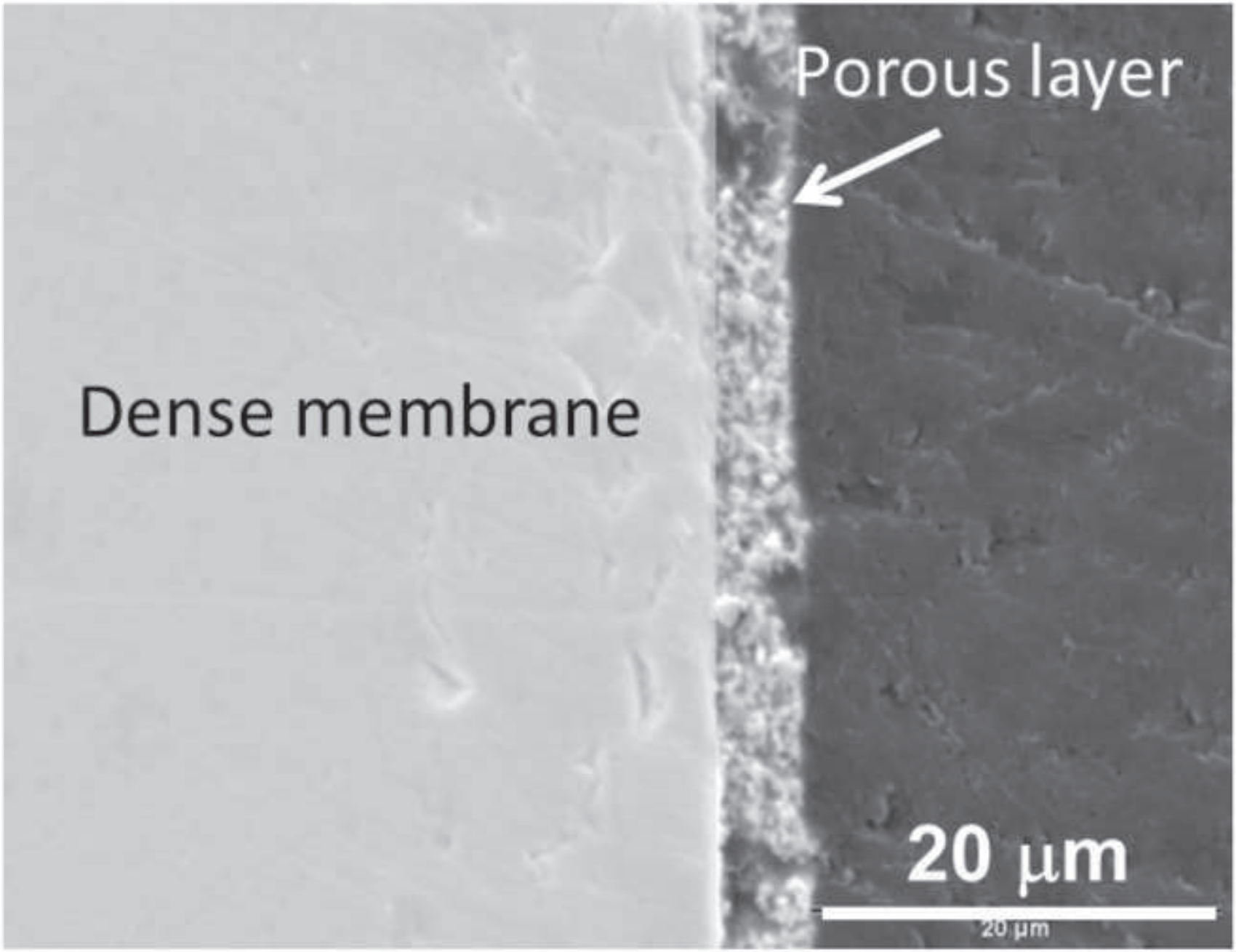

Figure 3

Click here to download high resolution image

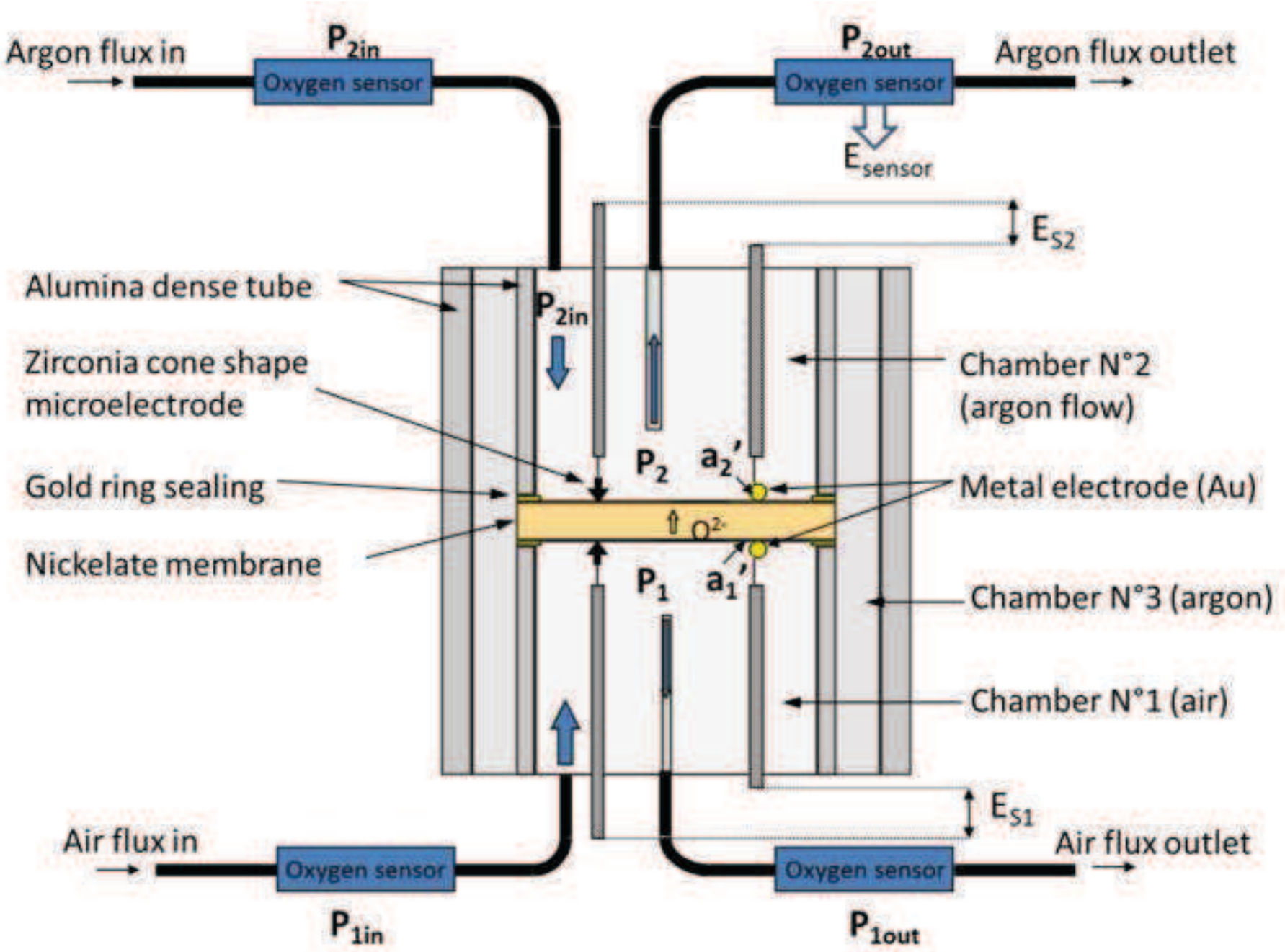

Figure 4

Click here to download high resolution image

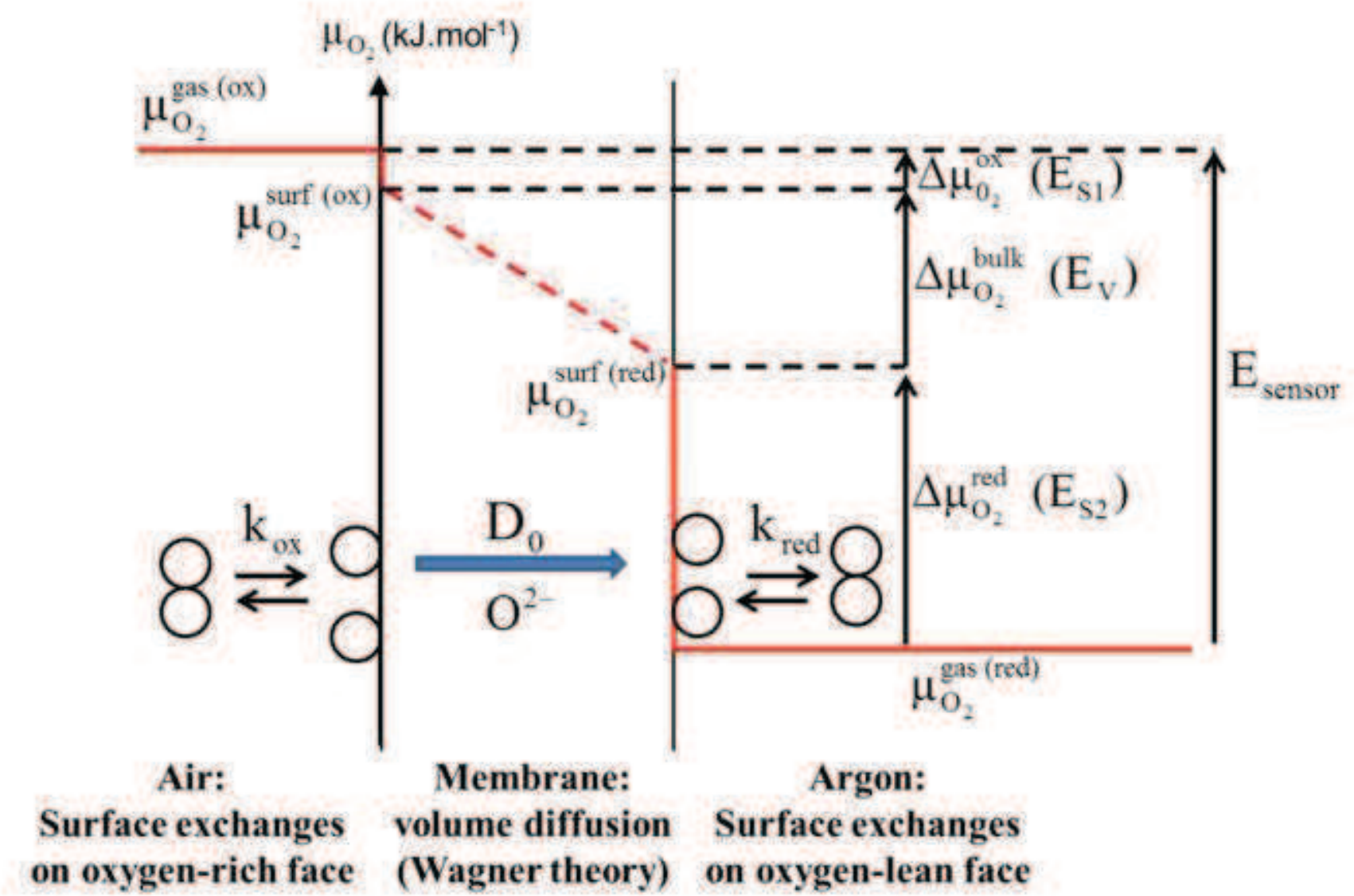

Figure 5

Click here to download high resolution image

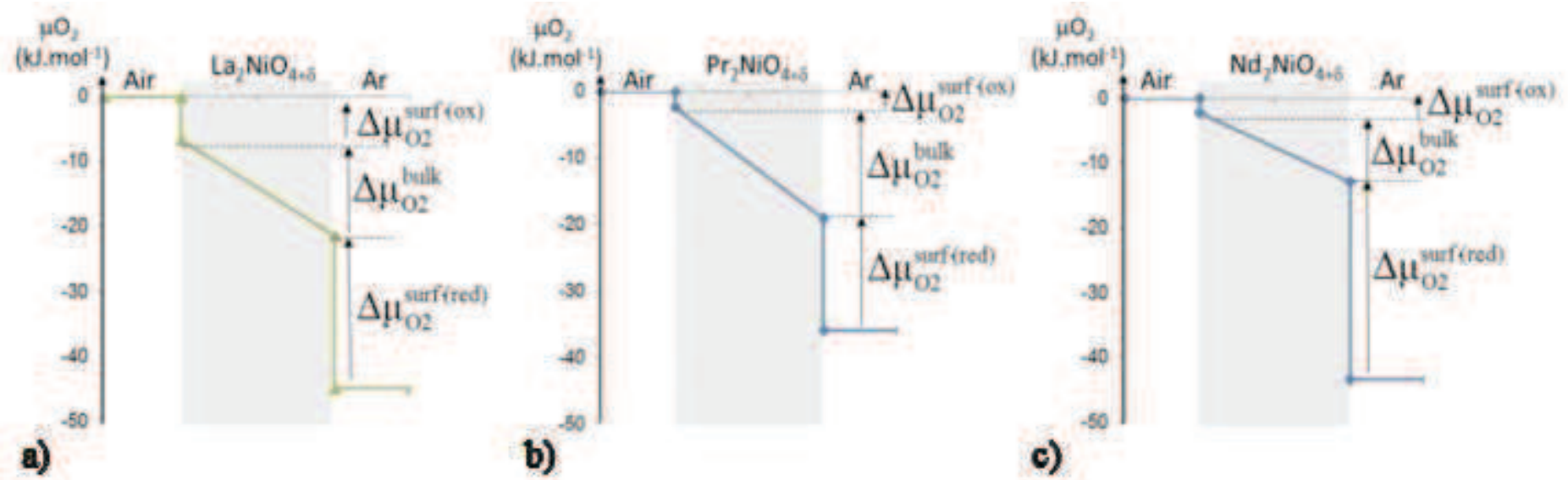

Figure 6
Click here to download high resolution image

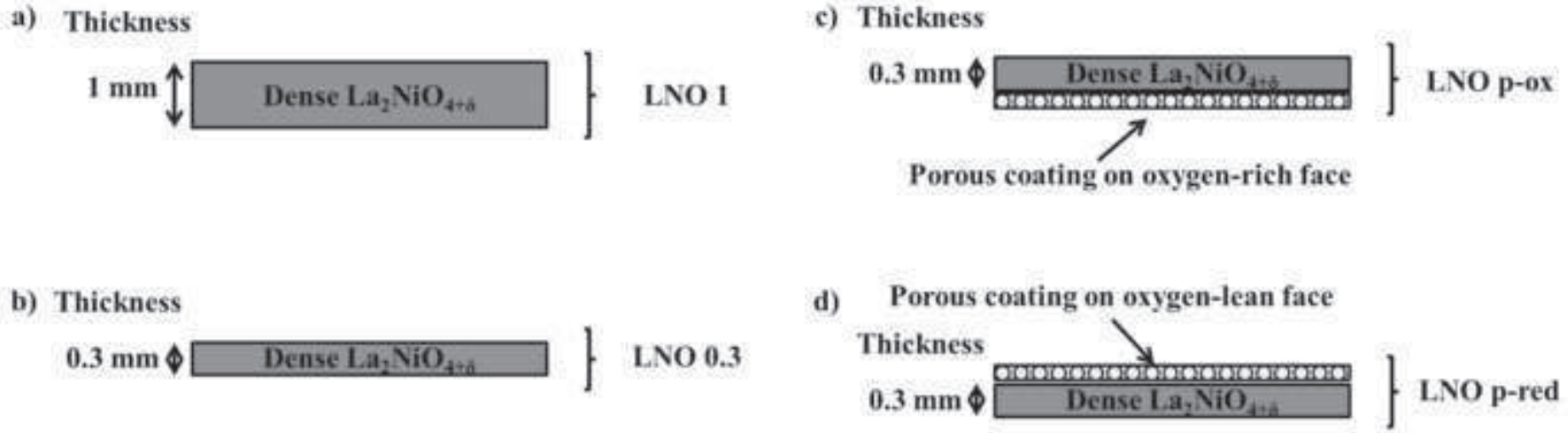

Figure 7
Click here to download high resolution image

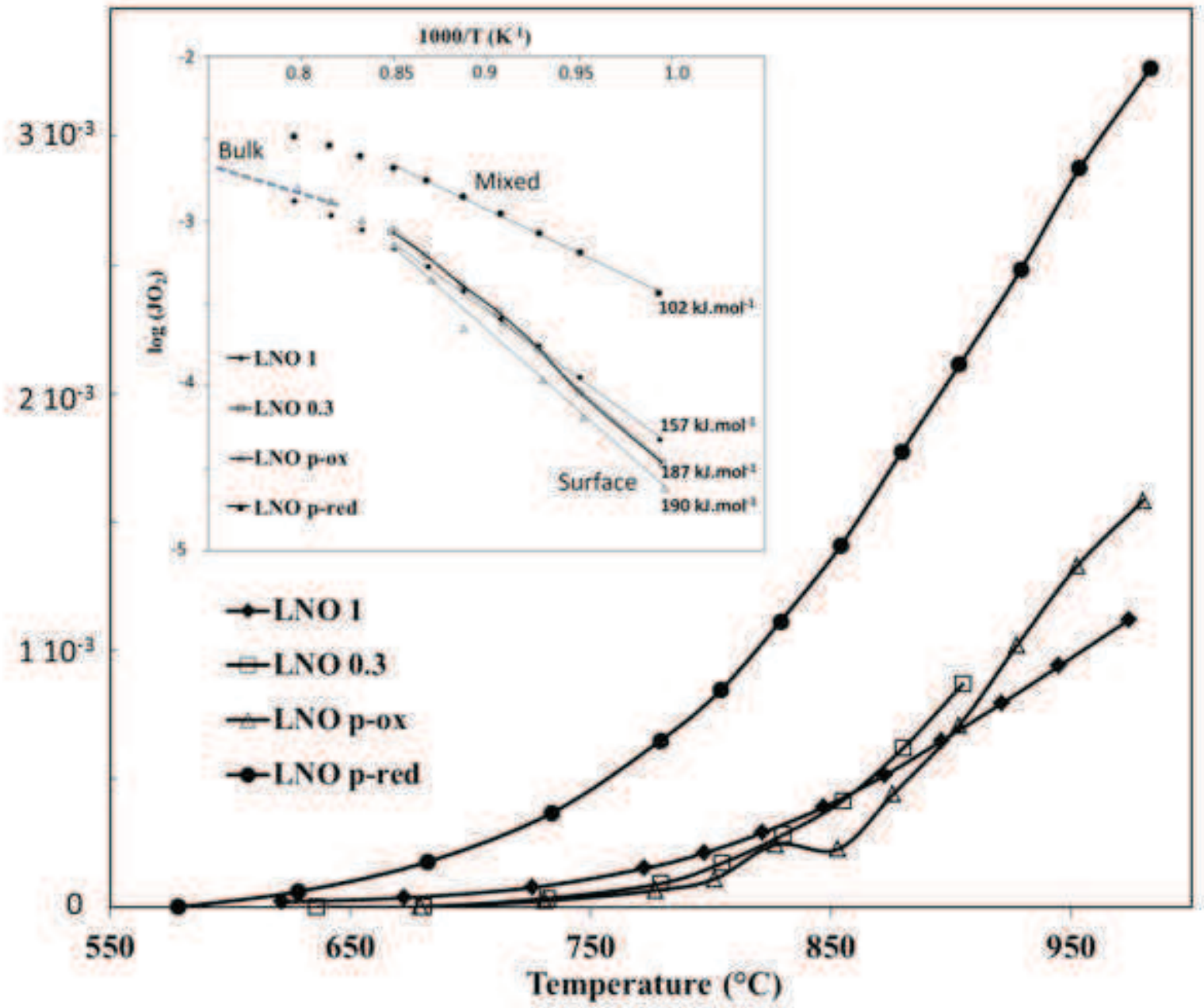

Figure 8
Click here to download high resolution image

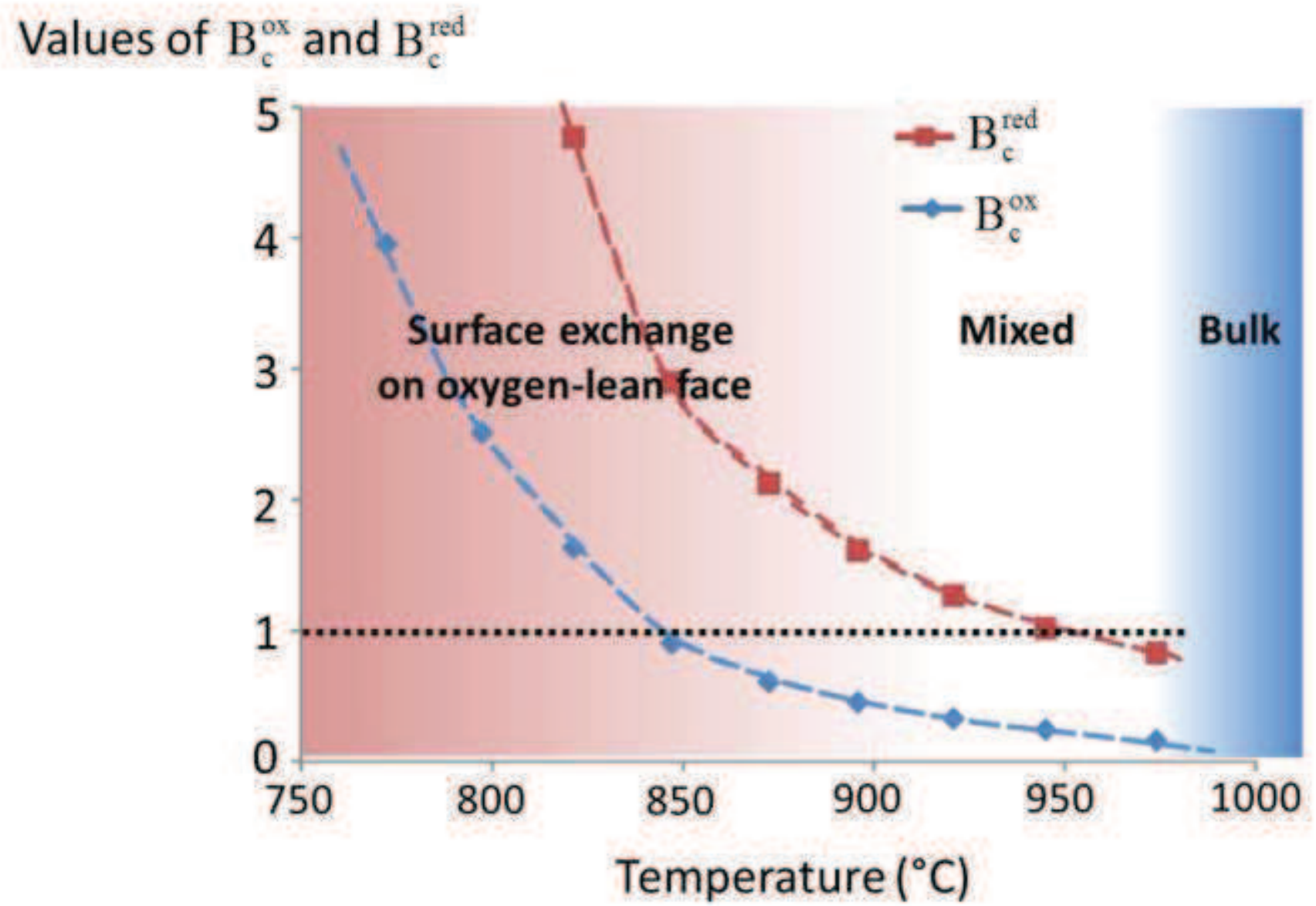

Figure 9

Click here to download high resolution image

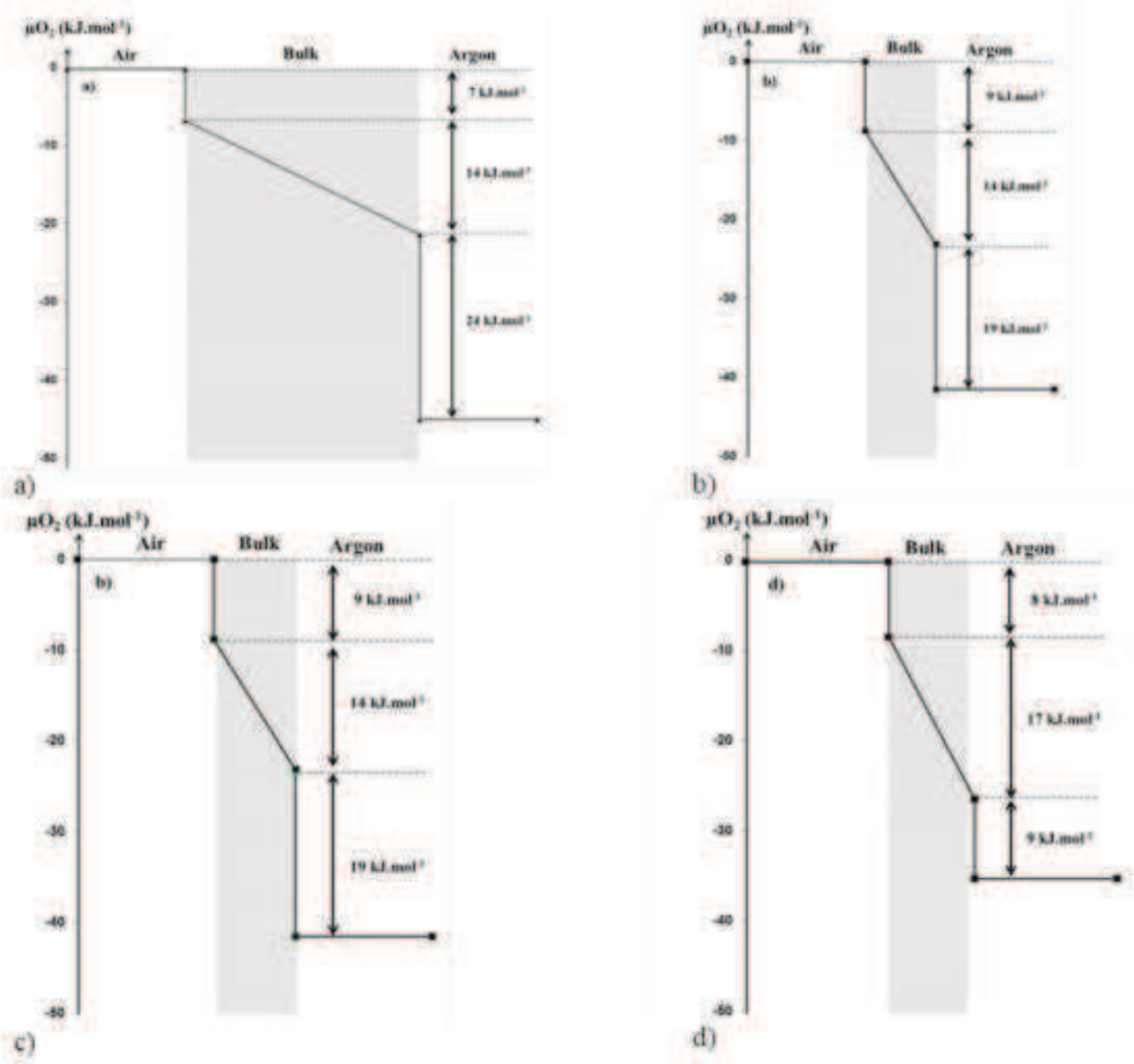

Table 1

Membrane materials	Density of starting powder (pycnometer)	Sintering thermal treatment	Density of sintered sample (Archimede method)	Relative density of sintered sample	Mean grain size
$La_2NiO_{4+\delta}$	6.78 $g.cm^{-3}$	1375°C, 1h, air	6.71	99%	1-3 µm
$Pr_2NiO_{4+\delta}$	7.16 $g.cm^{-3}$	1250°C, 1h, air	7.02	98%	0.5-1 µm
$Nd_2NiO_{4+\delta}$	7.14 $g.cm^{-3}$	1400°C, 1h, air	6.86	96%	2-4 µm

Table 1: Sintering thermal treatments and relative densities of the $Ln_2NiO_{4+\delta}$ membranes.

Table 2

Bc values	Rate determining step	Type of regime
$B_c << 1$	Oxygen bulk diffusion	Bulk
$B_c \approx 1$	Oxygen bulk diffusion and surface exchange	Mixed
$B_c >> 1$	Oxygen surface exchange	Surface

Table 2: Identification of the rate determining step of the oxygen flux from B_c values.

Table 3

Nickelate membranes at 900°C	**J_{O2} (mol. $m^2.s^{-1}$)**	**D_o ($cm^2.s^{-1}$)**	**k_{ex} on air side ($cm.s^{-1}$)**	$t_i = \frac{\sigma_i}{\sigma_e}$	$Lc = \frac{D^*}{k^*}$ (mm)	$B_c^{ox} = \frac{\Delta\mu_{O_2}^{ox\ surface}}{\Delta\mu_{O_2}^{bulk}}$	$B_c^{red} = \frac{\Delta\mu_{O_2}^{red\ surface}}{\Delta\mu_{O_2}^{bulk}}$	**Rate determining Step**
$La_2NiO_{4+\delta}$	7-8 10^{-4}	2-2.7 10^{-7} D*= 2 10^{-7}	4-9 10^{-6} k*=1 10^{-6}	1-1.5 10^{-3}	2	0.2-0.4	1.6-2.4	Surface exchange at oxygen-lean surface
$Pr_2NiO_{4+\delta}$	2 10^{-3}	2 10^{-6} D*= 2 10^{-7}	1-3 10^{-5} k*=4 10^{-6}	6.7 10^{-4}	0.5	0.14	1.0	Surface exchange at oxygen-lean surface + volume
$Nd_2NiO4_{+\delta}$	1 10^{-3}	1-4 10^{-7} D*= 4 10^{-7}	3-6 10^{-7} k*=4 10^{-6}	0.8-1.8 10^{-3}	1	0.2	3-3.2	Surface exchange at oxygen-lean surface

Table 3: The D_o and k_{ex} values at 900°C have been calculated from the relationships eq. 5, 6 and 9. D* and k* have been estimated from data of Boehm *et al.* [6, 27].

Table 4

Nickelate membranes at 800°C	**J_{O2} (mol. $m^2.s^{-1}$)**	**D_O ($cm^2.s^{-1}$)**	**k_{ex} on air side ($cm.s^{-1}$)**	$t_i = \frac{\sigma_i}{\sigma_e}$	$Lc = \frac{D^*}{k^*}$ (mm)	$B_c^{ox} = \frac{\Delta\mu_{O_2}^{ox\ surface}}{\Delta\mu_{O_2}^{bulk}}$	$B_c^{red} = \frac{\Delta\mu_{O_2}^{red\ surface}}{\Delta\mu_{O_2}^{bulk}}$	**Rate determining Step**
$La_2NiO_{4+\delta}$	$1.5\text{-}2\ 10^{-4}$	$1\text{-}2\ 10^{-7}$ $D^*= 1.5\ 10^{-7}$ [6, 27] $D^*= 1.7\ 10^{-7}$ [3] $D^*= 0.5\ 10^{-7}$ [28, 29]	$0.8\text{-}2\ 10^{-6}$ $k^*=9\ 10^{-7}$ [6, 27] $k^*= 2.5\ 10^{-6}$ [3] $k^*= 1\ 10^{-6}$ [28]	$0.8\text{-}1.2\ 10^{-3}$	0.5-1.7	0.5	7-7.5	surface exchange at oxygen-lean surface
$Pr_2NiO_{4+\delta}$	$3\ 10^{-4}$	$2\ 10^{-7}$ $D^*= 1.5\ 10^{-7}$ [6, 27]	$7\text{-}9\ 10^{-6}$ $k^*=4\ 10^{-6}$ [6, 27]	$6\ 10^{-4}$	4	0.09	1.8	surface exchange at oxygen-lean surface
$Nd_2NiO_{4+\delta}$	$0.3\text{-}3\ 10^{-4}$	$0.14\text{-}2\ 10^{-7}$ $D^*= 1.5\ 10^{-7}$ [6, 27]	$0.8\text{-}1.5\ 10^{-6}$ $k^*=3\ 10^{-6}$ [6, 27]	$0.12\text{-}2\ 10^{-3}$	0.5	0.5	6.5	surface exchange at oxygen-lean surface

Table 4: The D_O and k_{ex} values at 800°C have been calculated from the relationships eq. 5, 6 and 9 and data from refs. [3, 6, 27, 28, 29]

Table 5

$La_2NiO_{4+\delta}$	Thickness (mm)	Temperature (°C)	Gradient P_1/P_2 (atm)	$P_{O_2}^{red}$ (atm)	J_{O_2} ($mol.m^{-2}.s^{-1}$)	Shaping method	Type of sealing
Ref. [9]	0.35	850	0.21/ -	$1.7*10^{-3}$	$9.6*10^{-4}$	Tape casting	Not mentioned
This work	0.30	855	0.22/ 7 10^{-6} (Ar)	$2*10^{-3}$	$8.8*10^{-4}$	Tape casting	Gold ring
Ref. [9]	1	850	0.21/ -	$1*10^{-2}$	$8.4*10^{-4}$	Uniaxial pressing	Not mentioned
This work	1	847	0.21/2 10^{-6} (Ar)	$1.2*10^{-3}$	$3.9*10^{-4}$	Tape casting	Gold ring
Ref. [9]	1	950	0.21/ -	$1.3*10^{-2}$	$1.1*10^{-3}$	Uniaxial pressing	Not mentioned
This work	1	945	0.21/2 10^{-6} (Ar)	$3*10^{-3}$	$9.4*10^{-4}$	Tape casting	Gold ring

Table 5 Comparative values of the oxygen flux obtained with LNO 1 and LNO 0.3 membranes [9].

Table 6

$La_2NiO_{4+\delta}$	Ea ($kJ.mol^{-1}$) 700 - 900°C
LNO 1	157
LNO 0.3	187
LNO p-ox	190
LNO p-red	102

Table 6 Activation energy (Ea) of the oxygen flux through the $La_2NiO_{4+\delta}$ designed membranes